Quantitative Structure–Property Relationship Studies on Ostwald Solubility and Partition Coefficients of Organic Solutes in Ionic Liquids

Alan R. Katritzky,*,[§] Minati Kuanar,[§] Iva B. Stoyanova-Slavova,[§] Svetoslav H. Slavov,[§] Dimitar A. Dobchev,[§,||] Mati Karelson,[||] and William E. Acree, Jr.[⊥]

Center for Heterocyclic Compounds, Department of Chemistry, University of Florida, Gainesville, Florida 32611, Department of Chemistry, Tallinn University of Technology, Akadeemia tee 15, Tallinn 12618, Estonia, and Department of Chemistry, University of North Texas, Denton, Texas 76203-5070

Interactions of solutes with diverse ionic liquid solvents have been investigated by quantitative structure–property relationship (QSPR) methodology. Ostwald solubility coefficients and partition coefficients of organic solutes in eight different ionic liquids are correlated by molecular descriptors calculated solely from their structures. Two- to four-parameter best multilinear regression models were obtained with coefficients of determination ranging from 0.913 to 0.992. Additionally, several models were obtained with the same descriptors for all eight ionic liquids (ILs). Charge-related type descriptors contributed significantly to most of the models. The QSPR models were validated using the leave-one-out cross validation method.

Introduction

Ionic liquids (ILs) are a class of novel compounds that are composed entirely of ions, contain at least one organic ion in an ion pair, and are liquid at or near room temperature. ILs have received a great deal of attention due to their unique properties such as solvation ability for a wide range of compounds, high thermal stability, electroconductivity, and very low vapor pressure.[1] Ionic liquids have found potential applications in "green" chemistries, separation processes, and various catalytic reactions.[2–4]

Experimental solubilities and infinite dilution activity coefficients, γ_i^∞, of solutes dissolved in ionic liquids are important properties, which describe solute–solvent interactions. These properties have practical applications in commercial processes involving chromatographic separations and liquid–liquid extractions. Several publications report limited experimental measurements of the infinite dilution activity coefficients,[5–12] γ_i^∞, and Henry's law constants[13,14] of various solutes in different ILs. However, the literature lacks data for the solubility of many common organic chemicals in ionic liquids. Hence, a quantitative structure–property relationship (QSPR) theoretical approach that would provide quantitative correlation and hence the possibility of prediction of solubilities in ionic liquids, together with additional physical properties, could benefit researchers in this area.

Quantitative structure–property relationship studies have found wide applications in various research areas of chemistry, as an efficient tool in the correlation and prediction of diverse physicochemical properties. Several physicochemical and biological properties such as aqueous solubilities, vapor pressures, water–air partition coefficients,[15,16] partitioning behavior of organic solutes in aqueous biphasic systems,[17] blood−air and tissue−air partition coefficients of organic solutes,[18,19] partition of drugs between human milk and plasma,[20] and blood-to-brain distribution coefficients of drugs[21] were investigated by our group.

In recent years, QSPR methodology has been employed for the correlation and prediction of various physicochemical properties of ionic liquids. Melting points of several imidazolium and pyridinium based ionic liquids were correlated by our group using molecular descriptors calculated by the CODESSA Pro program.[22,23] Previous QSPR models for the correlation of melting points of ionic liquids and related properties[24–28] included studies by Abraham and co-workers[29–31] based on linear free energy relationship (LFER) methods for the prediction of partition coefficients of various solutes in ionic liquids.

Gutowski et al.[32] have correlated the enthalpies of formation and stabilities of energetic ionic liquids by ab initio electronic structure calculations. Semiempirical methods including UNIFAC group contributions and COSMO-RS were applied to predict infinite dilution activity coefficients of ionic liquids.[33,34] Eike et al.[35] correlated infinite dilution activity coefficients for 38 solutes in three ionic liquids (1-butyl-4-methylpyridinium tetrafluoroborate, 1-methyl-3-ethylimidazolium bis(trifluoromethylsulfonyl)imide, and 1,2-dimethyl-3-ethylimidazolium bis(trifluoromethylsulfonyl)imide) with a correlation coefficients of 0.90 to 0.99 by QSPR methodology. Tamm and Burk[36] correlated the infinite dilution activity coefficients of three ionic liquids for the same set of 38 organic compounds with structural descriptors. QSPR models for the toxicity data of ionic liquids (log IC_{50} and log LC_{50}) were reported with an R^2 of 0.78 to 0.88.[37]

Our group reported a general treatment of solubility in traditional organic solvents.[38–40] In continuation of this earlier work, we have now attempted the correlation of the solubility of solutes in various ionic liquids. The present study develops QSPR models for the correlation of Ostwald solubility coefficients (log L) and partition coefficients (log P) of organic solutes in eight ionic liquids based on molecular descriptors calculated solely from the structure of a molecule.

* Corresponding author. Phone: (352) 392-0554. Fax: (352) 392-9199. E-mail: katritzky@chem.ufl.edu.
[§] University of Florida.
[||] Tallinn University of Technology.
[⊥] University of North Texas.

10.1021/je700607b CCC: $40.75 © 2008 American Chemical Society
Published on Web 04/22/2008

Data Set

The experimental data for the present work based on the infinite dilution activity coefficients of solutes in eight different ionic liquids, such as 1-methyl-3-ethylimidazolium bis(trifluoromethylsulfonyl)imide ($[meim]^+[Tf_2N]^-$) IL-I, 1,2-dimethyl-3-ethylimidazolium bis(trifluoromethylsulfonyl)imide ($[m_2eim]^+[Tf_2N]^-$) IL-II, 1-methyl-3-butylimidazolium bis(trifluoromethylsulfonyl)imide ($[mbim]^+[Tf_2N]^-$) IL-III, 1-methyl-3-hexylimidazolium bis(trifluoromethylsulfonyl)imide ($[mhim]^+[Tf_2N]^-$) IL-IV, trimethylbutylammonium bis(trifluoromethylsulfonyl)imide ($[m_3bam]^+[Tf_2N]^-$) IL-V, 1-methyl-3-octylimidazolium tetrafluoroborate ($[moim]^+[BF_4]^-$) IL-VI, 1-methyl-3-butylimidazolium hexafluorophosphate ($[mbim]^+[PF_6]^-$) IL-VII, and 4-methyl-*N*-butylpyridinium tetrafluoroborate ($[mbpy]^+[BF_4]^-$) IL-VIII, were collected from 20 literature sources.[5,6,8,10,12–14,34,41–52] Except for IL-VIII, which contains a pyridinium ring, all the ILs investigated are imidazoliums. For ionic liquids I to V, the anion is bis(trifluoromethylsulfonyl)imide $[Tf_2N]^-$. For ILs VI and VIII, it is tetrafluoroborate $[BF_4]^-$, while IL-VII contains the hexafluorophosphate $[PF_6]^-$ counterion. Each data set contains 30 to 60 organic solutes.

For each of the eight ILs, the Ostwald solubility coefficients (log *L*) were computed by eq 1 for all 92 organic solutes with available data. In eq 1, γ_i^∞ is the infinite dilution activity coefficient; *p* is the vapor pressure of the solute at the system temperature; and *V* is the molar volume of the ionic liquid solvent.

$$\log L = \log(RT/\gamma_i^\infty pV) \quad (1)$$

$$\log P = \log L - \log L_W \quad (2)$$

The partition coefficients log *P* for the solutes in the eight ionic liquids were calculated by eq 2, where L_W is the Ostwald coefficient of the solute in water. The Ostwald solubility coefficients (log *L*) and partition coefficients (log *P*) were calculated by eqs 1 and 2.

Methodology

QSPR Modeling. The 2D-structures of the compounds were drawn using ChemDraw.[53] A three-dimensional conversion and preoptimization were performed using the molecular mechanics (MM+) implemented in the HyperChem 7.01 package.[54] Final geometry optimization of the molecules was carried out by using the semiempirical quantum-mechanical AM1 parametrization. A gradient norm 0.042 $kJ \cdot Å^{-1}$ was applied in the geometry optimization for all structures as a stopping criterion. The optimized geometries were then loaded into CODESSA Pro software.[55] The CODESSA Pro program was used to calculate up to 725 different molecular descriptors, derived from the molecular structure for each solute and classified as: (i) constitutional, (ii) geometrical, (iii) topological, (iv) charge-related, (v) quantum chemical, and (vi) thermodynamic.

The best multilinear regression (BMLR) procedure available in the framework of the CODESSA-Pro was used to find the best correlation models from selected noncollinear descriptors. After defining the descriptor space for the solutes, the BMLR procedure[56] was used to find the best correlation between the descriptors and property. The BMLR selects the best two-parameter regression equations, then the best three-parameter regression equations, etc., on the basis of the highest R^2 and *F* values in a stepwise regression procedure. The result obtained by BMLR is the "best" representation of the property in the given descriptors pool. To develop QSPR models, it is important to decide when to stop the addition of descriptors during the stepwise regression procedure. An excessive number of descriptors could lead to overparameterized equations that are difficult to interpret in terms of interactions and mechanisms. Based on the variation of R^2, R^2_{cv}, and *F* values with respect to the number of descriptors in the equation, the optimum regression model was selected with the optimum low number of descriptors.

Results and Discussion

QSPR Modeling of Ostwald Solubility Coefficient (log L). The best three or four descriptor multilinear regression equations were developed for log *L* in eight ionic liquids. The statistical characteristics for each of these models are shown in Table 1. The BMLR method produced the best models in the respective descriptor spaces. To avoid the incorporation of collinear descriptors, a threshold value of $R^2_{intercorr.} \leq 0.5$ between the descriptors was set. Altogether, 16 different descriptors were involved in the QSPR models for the eight ILs I to VIII. The descriptor types include charge related (d_3, d_4, d_6, d_7, d_8, d_{22}, d_{26}, and d_{27}), geometrical (d_5, d_{24}), topological (d_{14}, d_{25}), and quantum mechanical (d_{17},d_{18}, d_{19}, and d_{28}). Their occurrence in the BMLR models is listed in Table 2. The coefficients of determination R^2 for the models reported ranged from 0.919 to 0.992, and variances s^2 ranged from 0.012 to 0.069 (Table 1). These parameters indicate satisfactory quality of the regressions.

The most important descriptors involved in the log *L* models depict the charge distribution within the molecules, which is a main factor describing the electrostatic interactions between the solute and the IL (see Table 2). In general, log *L* increases with increasing hydrogen donor/acceptor ability of the solute. The above conjectures are supported by the occurrences of the descriptors as given in Table 2, coupled with the positive contributions of the hydrogen bonding descriptors in the eqs in Table 1.

The descriptors *Information content parameter*, *Randic index*, and *Gravitational index* significantly contribute toward the solubility of organic solutes in ILs. They should account for the size and shape effects of the molecules in intermolecular interactions. The quantum mechanical descriptors d_{17} to d_{19} and d_{28} reflect the interatomic interactions averaged by the number of the atoms for a given molecule. The predicted values of log *L* for ILs I to IV are listed in Table 3, and the plot of the predicted versus observed plots for ILs I to IV is shown in Figure 1a to d (the remaining results for ILs V to VIII are given in Supporting Information SM1).

QSPR Modeling of Partition Coefficients (log P). A second goal of this investigation was to develop robust QSPR based on the BMLR method for partition coefficients (log *P*) defined by eq 2. The best two-parameter models found for the eight ILs are shown in Table 4a. Seven different descriptors (d_2, d_{11}, d_{12}, d_{13}, d_{15}, d_{16}, and d_{20}) were involved in the QSPR models for log *P* in the ILs-I to VIII. The descriptors *DPSA2 difference in CPSAs (PPSA2−PNSA2) Zefirov PC* d_2, and *Minimum partial charge (Zefirov)* for all atom types d_{12} are common to most of the equations. Table 4a demonstrates excellent correlations, with coefficients of determination R^2 from 0.913 to 0.987. The most significant parameter in these models is *Minimum partial charge (Zefirov) for all atom types* (d_{12}), which reflects the interaction of solutes and solvents (ILs). The cross-validated correlation coefficients R^2_{CV} (Table 4a) range from 0.896 to 0.986, suggesting good predictability for the equations. The leave-one-out algorithm was used for this validation. All descriptors involved in the QSPR models for log *P* are listed in Table 4b.

Table 1. Statistical Parameters for BMLR Models of Ostwald Solubility Coefficient (log *L*)[a]

property	BMLR equations	*n*	*k*	R^2	R^2_{cv}	*F*	s^2
log *L* (IL-I)	log *L* (IL-I) = −(0.968 ± 0.296) − (0.851 ± 0.040)d_{22} + (0.898 ± 0.049)d_{14} + (3.850 ± 0.229)d_8 − (0.209 ± 0.029)d_{18}	52	4	0.978	0.971	515.9	0.036
log *L* (IL-II)	log *L* (IL-II) = (0.445 ± 0.176) + (1.763 ± 0.113)d_7 + (0.0051 ± 0.0004)d_{24} − (3.265 ± 0.455)d_4 − (0.511 ± 0.079)d_{25}	38	4	0.934	0.901	117.0	0.048
log *L* (IL-III)	log *L* (IL-III) = −(4.192 ± 0.176) + (0.0022 ± 0.00004)d_5 + (1.534 ± 0.052)d_7 + (1.031 ± 0.042)d_{19} − (0.248 ± 0.028)d_{22}	57	4	0.992	0.990	1613.2	0.012
log *L* (IL-IV)	log *L* (IL-IV) = −(4.918 ± 0.334) + (0.0018 ± 0.0001)d_5 − (0.910 ± 0.053)d_{17} + (0.133 ± 0.011)d_3 + (0.202 ± 0.019)d_6	60	4	0.950	0.937	259.3	0.032
log *L* (IL-V)	log *L* (IL-V) = −(4.609 ± 0.297) + (0.0018 ± 0.0001)d_5 − (0.404 ± 0.024)d_{18} + (1.220 ± 0.081)d_7 + (0.107 ± 0.009)d_3	49	4	0.965	0.948	305.5	0.024
log *L* (IL-VI)	log *L* (IL-VI) = −(3.856 ± 0.242) + (0.0045 ± 0.0001)d_{24} + (1.918 ± 0.0701)d_7 + (0.861 ± 0.050)d_{19} + (0.0091 ± 0.0045)d_{26}	48	4	0.981	0.975	560.6	0.014
log *L* (IL-VII)	log *L* (IL-VII) = −(5.039 ± 0.368) − (1.051 ± 0.074)d_{22} + (1.144 ± 0.088)d_{19} − (0.0076 ± 0.0009)d_{28} + (21.495 ± 4.145)d_{27}	32	4	0.951	0.936	130.2	0.065
log *L* (IL-VIII)	log *L* (IL-VIII) = (0.511 ± 0.213) + (2.043 ± 0.136)d_7 + (0.0059 ± 0.0006)d_{24} − (0.6809 ± 0.0951)d_{25} − (2.787 ± 0.5498)d_4	38	4	0.919	0.878	93.3	0.069

[a] NB: number of data points (*n*), number of descriptors (*k*), squared correlation coefficient (R^2), cross validated squared correlation coefficient (R^2_{cv}), Fisher ratio (*F*), squared standard deviation (s^2).

Table 2. Descriptors Involved in the QSPR Models for log *L* in Eight ILs, I to VIII

descriptors	symbols	log *L* IL-I	log *L* IL-II	log *L* IL-III	log *L* IL-IV	log *L* IL-V	log *L* IL-VI	log *L* IL-VII	log *L* IL-VIII
average complementary information content (order 0)	d_{25}		×						×
count of H-donor sites (Zefirov PC) all	d_{26}						×		
DPSA3 difference in CPSAs (PPSA3-PNSA3) (Zefirov PC)	d_3				×	×			
FNSA-2 fractional PNSA (PNSA-2/TMSA) (MOPAC PC)	d_4		×						×
gravitation index (all atom pairs)	d_5			×	×	×			
gravitation index (all bonds)	d_{24}		×				×		×
HA dependent HDCA-1 (MOPAC PC)	d_6				×				
HA dependent HDCA-2 (MOPAC PC)	d_7		×	×		×	×		×
HA dependent HDSA-2/SQRT(TMSA) (Zefirov PC)	d_8	×							
HASA-2/TMSA (Zefirov PC)	d_{27}							×	
Randic index (order 3)	d_{14}	×							
total molecular 2-center exchange energy/# of atoms	d_{17}				×				
total molecular 2-center resonance energy	d_{28}							×	
total molecular 2-center resonance energy/# of atoms	d_{18}	×				×			
total molecular electrostatic interaction/# of atoms	d_{19}			×			×	×	
WNSA3 weighted PNSA (PNSA3*TMSA/1000) (Zefirov PC)	d_{22}	×		×				×	

Also, the predicted values of log *P* and the predicted vs observed plots for log *P* in ILs I to VIII are included in Supporting Information SM2.

Cross Validation. To validate the BMLR models developed for log *L* and log *P*, the parent data points were divided according to the experimental values into three subsets (A, B, C) as follows: the first, fourth, seventh, etc. data points comprise the first subset (A), the second, fifth, eighth, etc. comprise the second subset (B), and the third, sixth, ninth, etc. comprise the third subset (C). Three training sets were prepared as combinations of two subsets (A and B), (A and C), and (B and C). For each training set, the correlation equation was derived with the descriptors of the respective equations given in Tables 1 and 4a. The equations obtained were then used to predict log *L* and log *P* values for the compounds from the remaining test set (A, B, or C). The efficiency of QSPR models to predict log *L* and log *P* values was assessed by the squared correlation coefficients and standard deviations between experimental and predicted data for each test set (A, B, or C). The stability of the models is indicated by the close agreement of the average values of (i) R^2(Fit) and R^2(Pred) and (ii) the standard errors s^2(Fit) and s^2(Pred). For example, the R^2(Fit) values for log *L* ILs I to VIII range from 0.926 to 0.992, and R^2(Pred) values range from 0.908 to 0.990, respectively. The results from this validation are shown in Supporting Information SM3. These statistical parameters suggest good predictive power for each equation in log *L* and log *P*.

Common Descriptor Models for log L. One of the main goals of this work was also to generalize the QSPR representation of log *L* for all eight ILs. More precisely, we aimed to build a model with the same descriptors common for all eight ILs. To do this, we explored the occurrences of the descriptors in Table 2. The descriptors which appeared in the previous models were preselected. Thus, a smaller descriptor space was formed on which the BMLR was run for each IL. The best four-descriptor regression models for log *L* are reported in the Supporting Information (SM-4a): the four descriptors best describing the eight ILs as a group were: *DPSA3 difference in CPSAs (PPSA3-PNSA3) (Zefirov PC)* d_3, *Gravitation index (all atom pairs)*, d_5, *HA dependent HDCA-2 (MOPAC PC)* d_7, *Total molecular electrostatic interaction/number of atoms,* d_{19}. The statistical characteristics of the models are also shown in SM-4a. For ILs I to VIII, four descriptors (d_3, d_5, d_7, d_{19}) contributed to the model with an R^2 of 0.988 to 0.868 and R^2_{CV} of 0.984 to 0.778. Two of these descriptors, *Area weighted surface charge of hydrogen bonding donor atoms* d_7 and *Difference between atomic charge weighted part positive and negative surface areas* (d_3), are related to the charge distribution interaction between the solutes and the ionic liquids. Descriptor d_{19}, the *Total molecular electrostatic interaction per number of atoms* also has a significant role in the solute and solvent interactions. The geometrical descriptor d_5 reflects the molecular shape and mass distribution in the solute molecule.

Table 3. Experimental and Predicted Ostwald Solubility Coefficient (log *L*) Values Using BMLR Models in Four Different Ionic Liquids (ILs I to IV)[a]

Sl. no.	compd name	exptl log *L* (IL-I)	pred. log *L* (IL-I)	exptl log *L* (IL-II)	pred. log *L* (IL-II)	exptl log *L* (IL-III)	pred. log *L* (IL-III)	exptl log *L* (IL-IV)	pred. log *L* (IL-IV)
1	Hexane	1.242	1.170	1.210	1.121	1.435	1.389	1.660	1.648
2	Heptane	1.572	1.526	1.557	1.571	1.785	1.790	2.041	2.046
3	Octane	1.895	1.697	1.891	1.823	2.128	2.134	2.415	2.383
4	Nonane	2.201	2.038	2.206	2.267	2.470	2.528	2.751	2.782
5	Decane	2.481	2.221	2.514	2.560	2.862	2.874	3.121	3.126
6	Cyclohexane	1.676	1.748	1.624	1.389	1.845	1.869	2.002	2.025
7	2,2,4-Trimethylpentane	1.563	1.418	1.548	1.978		2.456		2.601
8	Cyclohexene	2.001	2.005	1.961	1.903	2.130	2.146	2.260	2.347
9	Styrene	3.852	3.802	3.874	3.735		3.849		4.016
10	Benzene	2.812	2.801	2.814	2.736	2.883	3.035	2.886	3.243
11	Toluene	3.166	3.066	3.159	3.107	3.203	3.222	3.300	3.387
12	Ethylbenzene	3.417	3.340	3.389	3.377	3.474	3.439	3.569	3.598
13	*o*-Xylene	3.659	3.553	3.665	3.424		3.501		3.607
14	*p*-Xylene	3.486	3.359	3.474	3.382		3.471	3.663	3.602
15	*m*-Xylene	3.498	3.214	3.485	3.316		3.460	3.688	3.588
16	Isopropylbenzene	3.560	3.602	3.512	3.772		3.789		3.903
17	*tert*-Butylbenzene	3.785	3.823	3.727	4.178		4.222		4.273
18	Methanol	2.655	2.883	2.510	2.760	2.589	2.583	2.478	2.408
19	Ethanol	2.855	2.710	2.693	2.844	2.756	2.789	2.659	2.719
20	1-Propanol	3.167	3.252	3.008	3.020	3.052	3.084	3.016	3.080
21	1-Butanol	3.507	3.600	3.352	3.385	3.507	3.494	3.498	3.576
22	1-Pentanol	3.766	3.948	3.604	3.600	3.910	3.823	3.841	3.909
23	1-Hexanol	4.152	4.276	4.406	4.007	4.306	4.234	4.268	4.348
24	2-Propanol	2.863	2.613	2.712	2.914	2.831	2.958	2.797	2.849
25	*tert*-Butanol	2.911	2.549	2.767	3.129	2.902	3.263	2.876	3.096
26	2-Butanol	3.164	3.298	3.020	3.021	3.150	3.183	3.136	3.012
27	2-Methyl-2-butanol	3.251	3.268	3.101	3.107	3.286	3.376	3.303	3.091
28	Cyclohexanol	4.502	4.260	4.353	3.924	4.462	4.442	4.336	4.218
29	Acetonitrile	3.250	2.987	3.197	2.829	3.164	2.912	3.124	2.793
30	Acetone	2.902	2.998	2.804	2.897	2.873	2.666	2.848	2.726
31	Ethyl acetate	2.950	2.746	2.830	2.937		3.099		3.119
32	Dichloromethane	2.231	2.229	2.217	2.200		1.080		1.839
33	Trichloromethane	2.590	2.486	2.565	2.414		2.208	2.643	2.294
34	Tetrachloromethane	2.289	2.117	2.226	2.555		3.396		2.515
35	1-Methylcyclohexene	2.269	2.384	2.234	2.225		2.520		2.690
36	α-Methylstyrene	4.086	3.948	4.143	4.157		4.108		4.205
37	Methyl *tert*-butyl ether	2.073	2.000	1.958	1.890		2.184		2.394
38	Methyl *tert*-amyl ether	2.393	2.481	2.269	2.127		2.511		2.653
39	Anisole	4.081	4.107		4.009		4.274		4.326
40	Benzyl alcohol	5.580	5.712		5.835		5.948		5.744
41	Ethyl benzoate	5.021	5.531		5.986		5.930		5.730
42	Cyclopentane	1.338	1.556		1.145	1.517	1.464	1.678	1.674
43	1-Pentene	1.133	1.212		1.395	1.300	1.272	1.432	1.582
44	1-Hexene	1.476	1.512		1.754	1.652	1.630	1.826	1.932
45	1-Heptene	1.796	1.749		2.049	1.996	1.974	2.191	2.266
46	2-Butanone	3.201	3.377		2.971		2.900		2.914
47	2-Pentanone	3.455	3.450		3.239		3.220	3.505	3.246
48	Cyclopentene	1.552	1.856		1.741	1.678	1.795		2.046
49	Ethane	−0.169	0.074		0.053	−0.058	−0.253		0.005
50	Ethene	−0.011	0.497		0.646	0.084	0.221		0.654
51	Propane	0.205	0.235		0.338	0.292	0.233		0.504
52	Propene	0.449	0.512		0.880	0.581	0.591		0.937
53	Butane		0.701		0.537	0.691	0.631		0.896
54	Pentane		0.997		0.916	1.090	1.038	1.232	1.299
55	Undecane		2.541		2.989	3.218	3.261	3.499	3.513
56	Dodecane		2.711		3.290	3.573	3.604	3.874	3.854
57	Cycloheptane		1.978		1.711		2.293	2.583	2.421
58	1,3-Cyclohexadiene		2.297		2.304	2.398	2.495	2.489	2.717
59	1-Butene		1.003		1.139	0.925	0.931		1.255
60	1-Octene		2.032		2.411	2.337	2.334	2.559	2.621
61	1-Nonene		2.260		2.729	2.680	2.681	2.887	2.954
62	1-Dodecene		3.073		3.840	3.639	3.769	3.864	4.027
63	1-Hexyne		1.732		2.278		1.927	2.348	2.175
64	1-Heptyne		1.942		2.557		2.223	2.856	2.458
65	1-Octyne		2.218		2.947		2.551	3.136	2.772
66	Propylbenzene		3.398		3.693	3.754	3.692	3.872	3.841
67	Butylbenzene		3.526		3.935	4.099	3.948	4.242	4.075
68	Pentylbenzene		3.747		4.251	4.466	4.247	4.708	4.379
69	1-Heptanol		4.581		4.296	4.764	4.580		4.668
70	2-Methyl-1-propanol		3.300		3.261	3.324	3.387	3.319	3.318
71	Propanal		3.472		2.781	2.602	2.675	2.590	2.779
72	Butanal		3.797		2.943	2.922	2.905	2.942	3.026
73	Pentanal		4.207		3.219	3.101	3.227	3.154	3.364
74	Hexanal		4.534		3.522	3.651	3.577	3.716	3.701
75	Heptanal		4.915		3.842	4.028	3.942	4.076	4.052
76	Octanal		5.259		4.177	4.350	4.317	4.452	4.396
77	Methyl propanoate		2.981		2.895	2.969	3.068	2.998	3.036
78	Methyl butanoate		3.292		3.161	3.271	3.365	3.313	3.444

Table 3. Continued

Sl. no.	compd name	exptl log *L* (IL-I)	pred. log *L* (IL-I)	exptl log *L* (IL-II)	pred. log *L* (IL-II)	exptl log *L* (IL-III)	pred. log *L* (IL-III)	exptl log *L* (IL-IV)	pred. log *L* (IL-IV)
79	Methyl pentanoate		3.522		3.420	3.598	3.629	3.689	3.747
80	Methyl hexanoate		3.928		3.730	3.865	3.968	3.934	4.131
81	Diisopropyl ether		1.638		2.134		2.430	2.147	2.567
82	Ethyl *tert*-butyl ether		1.498		2.023		2.420		2.522
83	Ethyl *tert*-amyl ether		2.324		2.415		2.858	2.629	2.949
84	Tetrahydrofuran		2.448		1.816		2.249	2.866	2.535
85	1,4-Dioxane		3.512		2.715	3.506	3.431		3.692
86	Carbon tetrachloride		2.117		2.555		3.396	2.474	2.515
87	Methane		−0.089		−0.030		−0.881		−0.578
88	Diethyl ether		1.526		1.426		1.650		1.891
89	1-Nitropropane		2.623		3.617		3.663		2.887
90	Triethylamine		2.984		2.695		2.937		2.802
91	Pyridine		4.485		4.683		4.983		4.674
92	Thiophene		4.040		3.311		2.455		3.269

[a] NB: IL-I $[meim]^+[Tf_2N]^-$ is 1-methyl-3-ethylimidazolium bis(trifluoromethylsulfonyl)imide; IL-II $[mmeim]^+[Tf_2N]^-$ is 1,2-dimethyl-3-ethylimidazolium bis(trifluoromethylsulfonyl)imide; IL-III $[mbim]^+[Tf_2N]^-$ is 1-methyl-3-butylimidazolium bis(trifluoromethylsulfonyl)imide, IL-IV $[mhim]^+[Tf_2N]^-$ is 1-methyl-3-hexylimidazolium bis(trifluoromethylsulfonyl)imide.

Table 4a. Statistical Parameters for BMLR Models of Partition Coefficients (log *P*)

property	BMLR equations	*n*	*k*	R^2	R^2_{cv}	*F*	s^2
log *P* (IL-I)	log *P* (IL-I) = −(1.335 ± 0.255) + (13.899 ± 0.673)d_{12} + (0.015 ± 0.001)d_{16}	52	2	0.951	0.945	478.8	0.106
log *P* (IL-II)	log *P* (IL-II) = (1.823 ± 0.118) + (22.548 ± 0.577)d_{12} + (0.031 ± 0.002)d_2	38	2	0.980	0.975	836.3	0.061
log *P* (IL-III)	log *P* (IL-III) = (0.466 ± 0.092) + (0.162 ± 0.004)d_{20} + (15.565 ± 0.429)d_{12}	56	2	0.987	0.986	2008.5	0.043
log *P* (IL-IV)	log *P* (IL-IV) = (1.121 ± 0.155) + (17.194 ± 0.700)d_{12} + (0.105 ± 0.005)d_{11}	60	2	0.965	0.961	785.8	0.123
log *P* (IL-V)	log *P* (IL-V) = (2.064 ± 0.097) + (23.188 ± 0.518)d_{12} + (0.027 ± 0.001)d_2	48	2	0.985	0.982	1472.1	0.056
log *P* (IL-VI)	log *P* (IL-VI) = (2.213 ± 0.111) + (22.638 ± 0.605)d_{12} + (0.031 ± 0.001)d_2	47	2	0.982	0.979	1182.7	0.075
log *P* (IL-VII)	log *P* (IL-VII) = (1.060 ± 0.309) + (18.672 ± 1.418)d_{15} + (0.071 ± 0.010)d_{12}	30	2	0.913	0.896	141.0	0.218
log *P* (IL-VIII)	log *P* (IL-VIII) = (1.891 ± 0.116) + (21.264 ± 0.564)d_{12} + (0.027 ± 0.002)d_2	38	2	0.978	0.973	768.8	0.058

Table 4b. Descriptors Involved in the QSPR Models for log *P* in Eight ILs I to VIII

descriptors	symbols	log *P* IL-I	log *P* IL-II	log *P* IL-III	log *P* IL-IV	log *P* IL-V	log *P* IL-VI	log *P* IL-VII	log *P* IL-VIII
DPSA2 difference in CPSAs (PPSA2-PNSA2) (Zefirov PC)	d_2		×			×	×		×
internal heat capacity (300 K)	d_{11}				×				
min. partial charge (Zefirov) for all atom types	d_{12}	×	×	×	×	×	×	×	×
PPSA2 total charge weighted PPSA (Zefirov PC)	d_{13}								
shadow plane ZX	d_{15}							×	
TMSA total molecular surface area (Zefirov PC)	d_{16}	×							
total number of atoms	d_{20}			×					

Similar general four-descriptor models were reported by Eike et al.[35] for the prediction of infinite dilution activity coefficients ($\ln \gamma_i^\infty$) in three ionic liquids, 1-butyl-4-methylpyridinium tetrafluoroborate, 1-methyl-3-ethylimidazolium bis(trifluoromethylsulfonyl)imide, and 1,2-methyl-3-ethylimidazolium bis(trifluoromethylsulfonyl)imide. The authors used calculated octanol–water partition coefficients [log K_{OW}], hydrogen bond donor counts [Hbonds], surface weighted partial negative surface area [$WNSA_1$], and electrotopological state indices [SaaCH]. Similar descriptors were also shown to have significant contributions in our models.

Common Descriptor Models for log P. The same general procedure, as described above for log *L*,was performed on the log *P* data. Overall, just two highly significant descriptors, i.e., *DPSA2 difference in CPSAs (PPSA2-PNSA2) Zefirov PC* d_2 and *Minimum partial charge (Zefirov) for all atom types* d_{12} contribute to all the eight models for log *P* (see SM-5a). Examination of the statistical parameters in SM-5a revealed that the equations for log *P* of ILs I to VIII have significant correlations with R^2 ranging from 0.904 to 0.985.

External Validation

The common descriptor models for log *L* and log *P* were externally validated for their predictive ability. Therefore, we divided the parent set into training and external test sets. Since the number of solutes in some ILs is low, we selected an external set for each IL with five to ten compounds. In the case of log *L*, the same four descriptors (d_3, d_5, d_7, and d_{19}) were used to build equations for the training sets (SM-4a) but with different regression coefficients. These equations were used for prediction of the respective test sets for each IL. The statistical characteristics of the validated models for log *L* are given in (SM-4b). Plots of predicted vs experimental

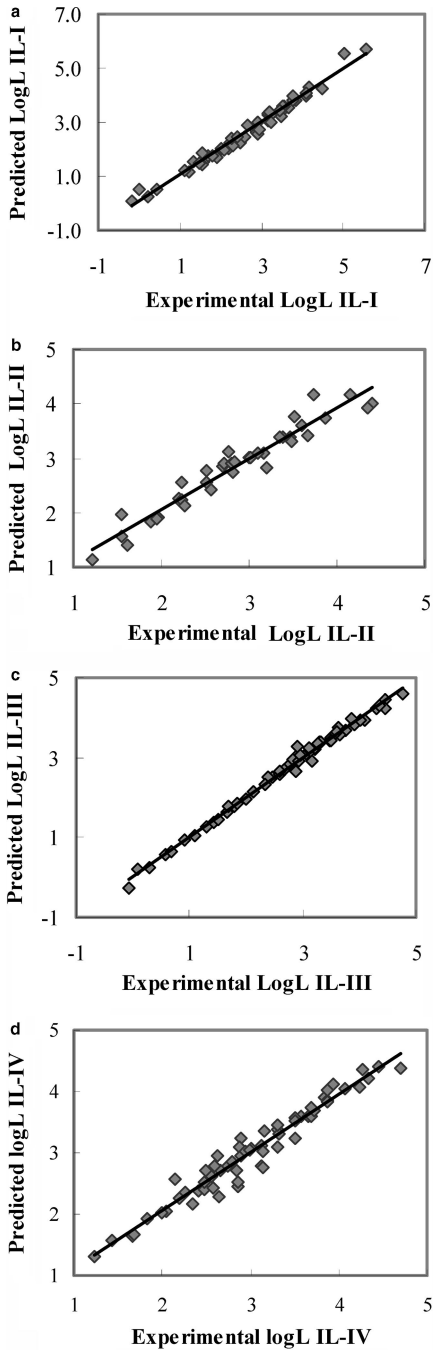

Figure 1. (a) Plot of predicted vs experimental log *L* values for IL-I for BMLR models. (b) Plot of predicted vs experimental log *L* values for IL-II for BMLR models. (c) Plot of predicted versus experimental log *L* values for IL-III for BMLR models. (d) Plot of predicted vs experimental log *L* values for IL-IV for BMLR models.

log *L* values in the eight ionic liquids (ILs I to VIII) are shown in SM 6, Figures I to VIII, for data points in the training set and for data points left out of the training set (external set). For most of the ILs, the external points were close to the regression line generated by the training set equations. However, in the ILs II and VIII, ethyl acetate deviated slightly from the line.

In the case of log *P* validation, the two descriptors (d_2 and d_{12}) were used in the models developed for log *P* for all the eight ILs (see SM-5a). For the external test sets, five to ten compounds were selected depending on the number of data points of the parent data sets. Significant QSPR equations were obtained for LogP in all the eight ILs I to VIII and are shown in (SM-5b).

Plots of the predicted vs experimental log *P* values for all eight ILs are given in SM-7. The compounds from the external (validation) data set fit well into the model derived for the training set.

Conclusions

Valid QSPR models, based on two to four molecular descriptors calculated solely from structure, were obtained for Ostwald solubility log *L* and partition coefficient log *P*. The parameters involved in the correlations reflect the physical significance of specific solute–solvent interactions for various solutes in ionic liquids.

Overall, the QSPR equations developed indicate the significant role in solvent–solute interactions and the charge-related descriptors alongside as the hydrogen donor/acceptor abilities of the solutes. In addition, the excellent predictive power of the models reported enabled highly accurate estimations of the log *L* and log *P* values for the external data sets.

The QSPR models developed herein should be useful for prediction of Ostwald solubility coefficients and partition coefficients of unknown solutes in ionic liquids. The common descriptor models developed could be used for the screening for suitable solutes in ionic liquids.

Supporting Information Available:

SM-1a to SM-7. This material is available free of charge via the Internet at http://pubs.acs.org.

Literature Cited

(1) Welton, T. Room-Temperature Ionic Liquids. Solvents for Synthesis and Catalysis. *Chem. Rev.* **1999**, *99*, 2071–2083.
(2) Sheldon, R. A.; Lau, R. M.; Sorgedrager, M. J.; van Rantwijk, F.; Seddon, K. R. Biocatalysis in Ionic Liquids. *Green Chem.* **2002**, *4*, 147–151.
(3) Dupont, J.; de Souza, R. F.; Suarez, P. A. Z. Ionic Liquid (Molten Salt) Phase Organometallic Catalysis. *Chem. Rev.* **2002**, *102*, 3667–3691.
(4) Seddon, K. R. Ionic Liquids for Clean Technology. *J. Chem. Technol. Biotechnol.* **1997**, *68*, 351–356.
(5) Heintz, A.; Kulikov, D. V.; Verevkin, S. P. Thermodynamic Properties of Mixtures Containing Ionic Liquids. Activity Coefficients at Infinite Dilution of Polar Solutes in 4-Methyl-N-butylpyridinium Tetrafluoroborate Using Gas-Liquid Chromatography. *J. Chem. Thermodyn.* **2002**, *34*, 1341–1347.
(6) Heintz, A.; Kulikov, D. V.; Verevkin, S. P. Thermodynamic Properties of Mixtures Containing Ionic Liquids. 1. Activity Coefficients at Infinite Dilution of Alkanes, Alkenes, and Alkylbenzenes in 4-Methyl-N-butylpyridinium Tetrafluoroborate Using Gas-Liquid Chromatography. *J. Chem. Eng. Data* **2001**, *46*, 1526–1529.
(7) Heintz, A.; Kulikov, D. V.; Verevkin, S. P. Thermodynamic Properties of Mixtures Containing Ionic Liquids. 2. Activity Coefficients at Infinite Dilution of Hydrocarbons and Polar Solutes in 1-Methyl-3-ethyl-imidazolium Bis(trifluoromethyl-sulfonyl)amide and in 1,2-Dimethyl-3-ethylimidazolium Bis(trifluoromethylsulfonyl)amide Using Gas−Liquid Chromatography. *J. Chem. Eng. Data* **2002**, *47*, 894–899.
(8) Krummen, N.; Wasserscheid, P.; Gmehling, J. Measurement of Activity Coefficients at Infinite Dilution in Ionic Liquids Using the Dilutor Technique. *J. Chem. Eng. Data* **2002**, *47*, 1411–1417.
(9) Warren, D.; Letcher, T. M.; Ramjugernath, D.; Raal, J. D. Activity Coefficients of Hydrocarbon Solutes at Infinite Dilution in the Ionic Liquid, 1-Methyl-3-octylimidazolium Chloride from Gas-Liquid Chromatography. *J. Chem. Thermodyn.* **2003**, *35*, 1335–1341.
(10) Heintz, A.; Verevkin, S. P.; Ondo, D. Thermodynamic Properties of Mixtures Containing Ionic Liquids. 8. Activity Coefficients at Infinite Dilution Of Hydrocarbons, Alcohols, Esters, and Aldehydes in 1-Hexyl-3-methylimidazolium Bis(trifluoromethylsulfonyl)imide Using Gas-Liquid Chromatography. *J. Chem. Eng. Data* **2006**, *51*, 434–437.

(11) Foco, G. M.; Bottini, S. B.; Quezada, N.; De la Fuente, J. C.; Peters, C. J. Activity Coefficients at Infinite Dilution in 1-Alkyl-3-methylimidazolium Tetrafluoroborate Ionic Liquids. *J. Chem. Eng. Data* **2006**, *51*, 1088–1091.

(12) Mutelet, F.; Butet, V.; Jaubert, J.-N. Application of Inverse Gas Chromatography and Regular Solution Theory for Characterization of Ionic Liquids. *Ind. Eng. Chem. Res.* **2005**, *44*, 4120–4127.

(13) Jacquemin, J.; Husson, P.; Majer, V.; Costa Gomes, M. F. Low-Pressure Solubilities and Thermodynamics of Solvation of Eight Gases in 1-Butyl-3-methylimidazolium Hexafluorophosphate. *Fluid Phase Equilib.* **2006**, *240*, 87–95.

(14) Anthony, J. L.; Maginn, E. J.; Brennecke, J. F. Solubilities and Thermodynamic Properties of Gases in the Ionic Liquid 1-N-Butyl-3-methylimidazolium Hexafluorophosphate. *J. Phys. Chem. B* **2002**, *106*, 7315–7320.

(15) Katritzky, A. R.; Mu, L.; Karelson, M. A QSPR Study of the Solubility of Gases and Vapors in Water. *J. Chem. Inf. Comput. Sci.* **1996**, *36*, 1162–1168.

(16) Katritzky, A. R.; Wang, Y.; Sild, S.; Tamm, T.; Karelson, M. QSPR Studies on Vapor Pressure, Aqueous Solubility, and the Prediction of Water-Air Partition Coefficients. *J. Chem. Inf. Comput. Sci.* **1998**, *38*, 720–725.

(17) Katritzky, A. R.; Taemm, K.; Kuanar, M.; Fara, D. C.; Oliferenko, A.; Oliferenko, P.; Huddleston, J. G.; Rogers, R. D. Aqueous Biphasic Systems. Partitioning of Organic Molecules: A QSPR Treatment. *J. Chem. Inf. Comput. Sci.* **2004**, *44*, 136–142.

(18) Katritzky, A. R.; Kuanar, M.; Fara, D. C.; Karelson, M.; Acree, W. E. QSPR Treatment of Rat Blood:Air, Saline:Air and Olive Oil:Air Partition Coefficients Using Theoretical Molecular Descriptors. *Bioorg. Med. Chem.* **2004**, *12*, 4735–4748.

(19) Katritzky, A. R.; Kuanar, M.; Fara, D. C.; Karelson, M.; Acree, W. E.; Solov'ev, V. P.; Varnek, A. QSAR Modeling of Blood:Air and Tissue: Air Partition Coefficients Using Theoretical Descriptors. *Bioorg. Med. Chem.* **2005**, *13*, 6450–6463.

(20) Katritzky, A. R.; Dobchev, D. A.; Huer, E.; Fara, D. C.; Karelson, M. QSAR Treatment of Drugs Transfer into Human Breast Milk. *Bioorg. Med. Chem.* **2005**, *13*, 1623–1632.

(21) Katritzky, A. R.; Kuanar, M.; Slavov, S.; Dobchev, D. A.; Fara, D. C.; Karelson, M.; Acree, W. E.; Solov'ev, V. P.; Varnek, A. Correlation of Blood-Brain Penetration Using Structural Descriptors. *Bioorg. Med. Chem.* **2006**, *14*, 4888–4917.

(22) Katritzky, A. R.; Lomaka, A.; Petrukhin, R.; Jain, R.; Karelson, M.; Visser, A. E.; Rogers, R. D. QSPR Correlation of The Melting Point for Pyridinium Bromides, Potential Ionic Liquids. *J. Chem. Inf. Comput. Sci.* **2002**, *42*, 71–74.

(23) Katritzky, A. R.; Jain, R.; Lomaka, A.; Petrukhin, R.; Karelson, M.; Visser, A. E.; Rogers, R. D. Correlation of the Melting Points of Potential Ionic Liquids (Imidazolium Bromides and Benzimidazolium Bromides) Using the CODESSA Program. *J. Chem. Inf. Comput. Sci.* **2002**, *42*, 225–231.

(24) Trohalaki, S.; Pachter, R.; Drake, G. W.; Hawkins, T. Quantitative Structure-Property Relationships for Melting Points and Densities of Ionic Liquids. *Energy Fuels* **2005**, *19*, 279–284.

(25) Eike, D. M.; Brennecke, J. F.; Maginn, E. J. Predicting Melting Points of Quaternary Ammonium Ionic Liquids. *Green Chem.* **2003**, *5*, 323–328.

(26) Carrera, G.; Aires-de-Sousa, J. Estimation of Melting Points of Pyridinium Bromide Ionic Liquids with Decision Trees and Neural Networks. *Green Chem.* **2005**, *7*, 20–27.

(27) Varnek, A.; Kireeva, N.; Tetko, I. V.; Baskin, I. I.; Solov'ev, V. P. Exhaustive QSPR Studies of a Large Diverse Set of Ionic Liquids: How Accurately Can We Predict Melting Points. *J. Chem. Inf. Model* **2007**, *47*, 1111–1122.

(28) Lopez-Martin, I.; Burello, E.; Davey, P. N.; Seddon, K. R.; Rothenberg, G. Anion and Cation Effects on Imidazolium Salt Melting Points: a Descriptor Modelling Study. *Chem. Phys. Chem.* **2007**, *8*, 690–695.

(29) Abraham, M. H.; Zissimos, A. M.; Huddleston, J. G.; Willauer, H. D.; Rogers, R. D.; Acree, W. E., Jr. Some Novel Liquid Partitioning Systems: Water-Ionic Liquids and Aqueous Biphasic Systems. *Ind. Eng. Chem. Res.* **2003**, *42*, 413–418.

(30) Acree, W. E., Jr.; Abraham, M. H. The Analysis of Solvation in Ionic Liquids and Organic Solvents Using the Abraham Linear Free Energy Relationship. *J. Chem. Technol. Biotechnol.* **2006**, *81*, 1441–1446.

(31) Sprunger, L.; Clark, M.; Acree, W. E., Jr.; Abraham, M. H. Characterization of Room-Temperature Ionic Liquids by the Abraham Model with Cation-Specific and Anion-Specific Equation Coefficients. *J. Chem. Inf. Model* **2007**, *47*, 1123–1129.

(32) Gutowski, K. E.; Holbrey, J. D.; Rogers, R. D.; Dixon, D. A. Prediction of the Formation and Stabilities of Energetic Salts and Ionic Liquids Based on ab Initio Electronic Structure Calculations. *J. Phys. Chem. B* **2005**, *109*, 23196–23208.

(33) Diedenhofen, M.; Eckert, F.; Klamt, A. Prediction of Infinite Dilution Activity Coefficients of Organic Compounds in Ionic Liquids Using COSMO-RS. *J. Chem. Eng. Data* **2003**, *48*, 475–479.

(34) Kato, R.; Gmehling, J. Systems with Ionic Liquids: Measurement of VLE and $\Gamma\infty$ Data and Prediction of their Thermodynamic Behavior Using Original UNIFAC, mod. UNIFAC (Do) and COSMO-RS(OI). *J. Chem. Thermodyn.* **2005**, *37*, 603–619.

(35) Eike, D. M.; Brennecke, J. F.; Maginn, E. J. Predicting Infinite-Dilution Activity Coefficients of Organic Solutes in Ionic Liquids. *Ind. Eng. Chem. Res.* **2004**, *43*, 1039–1048.

(36) Tamm, K.; Burk, P. QSPR Analysis for Infinite Dilution Activity Coefficients of Organic Compounds. *J. Mol. Model* **2006**, *12*, 417–421.

(37) Couling, D. J.; Bernot, R. J.; Docherty, K. M.; Dixon, J. K.; Maginn, E. J. Assessing the Factors Responsible for Ionic Liquid Toxicity to Aquatic Organisms Via Quantitative Structure-Activity Relationship Modeling. *Green Chem.* **2006**, *8*, 82–90.

(38) Katritzky, A. R.; Oliferenko, A. A.; Oliferenko, P. V.; Petrukhin, R.; Tatham, D. B.; Maran, U.; Lomaka, A.; Acree, W. E., Jr. A General Treatment of Solubility. 1. The QSPR Correlation of Solvation Free Energies of Single Solutes in Series of Solvents. *J. Chem. Inf. Comput. Sci.* **2003**, *43*, 1794–1805.

(39) Katritzky, A. R.; Oliferenko, A. A.; Oliferenko, P. V.; Petrukhin, R.; Tatham, D. B.; Maran, U.; Lomaka, A.; Acree, W. E., Jr. A General Treatment of Solubility. 2. QSPR Prediction of Free Energies of Solvation of Specified Solutes in Ranges of Solvents. *J. Chem. Inf. Comput. Sci.* **2003**, *43*, 1806–1814.

(40) Katritzky, A. R.; Tulp, I.; Fara, D. C.; Lauria, A; Maran, U.; Acree, W. E., Jr. A General Treatment of Solubility. 3. Principal Component Analysis (PCA) of the Solubilities of Diverse Solutes in Diverse Solvents. *J. Chem. Inf. Model* **2005**, *45*, 913–923.

(41) Heintz, A.; Vasiltsova, T. V.; Safarov, J.; Bich, E.; Verevkin, S. P. Thermodynamic Properties of Mixtures Containing Ionic Liquids. 9. Activity Coefficients at Infinite Dilution of Hydrocarbons, Alcohols, Esters, and Aldehydes in Trimethylbutylammonium Bis(trifluoromethylsulfonyl) Imide Using Gas-Liquid Chromatography and Static Method. *J. Chem. Eng. Data* **2006**, *51*, 648–655.

(42) Vasiltsova, T. V.; Verevkin, S. P.; Bich, E.; Heintz, A.; Bogel-Lukasil, R.; Domanska, U. Thermodynamic Properties of Mixtures Containing Ionic Liquids. Activity Coefficients of Ethers and Alcohols in 1-Methyl-3-ethylimidazolium Bis(trifluoromethylsulfonyl)imide Using the Transpiration Method. *J. Chem. Eng. Data* **2005**, *50*, 142–148.

(43) Vasiltsova, T. V.; Verevkin, S. P.; Bich, E.; Heintz, A.; Bogel-Lukasil, R.; Domanska, U. Thermodynamic Properties of Mixtures Containing Ionic Liquids. 7. Activity Coefficient of Aliphatic and Aromatic Esters and Benzylamine in 1-Methyl-3-ethylimidazolium Bis(trifluoromethyl)imide Using The Transpiration Method. *J. Chem. Eng. Data* **2006**, *51*, 213–218.

(44) Deenadayalu, N.; Letcher, T. M.; Reddy, P. Determination of Activity Coefficients at Infinite Dilution of Polar and Nonpolar Solutes in the Ionic Liquid 1-Ethyl-3-methylimidazolium Bis(trifluoromethylsulfonyl)imide Using Gas-Liquid Chromatography at the Temperature 303.15 or 318.15 K. *J. Chem. Eng. Data* **2005**, *50*, 105–108.

(45) Camper, D.; Becker, C.; Koval, C.; Nobel, R. Low Pressure Hydrocarbon Solubility in Room Temperature Ionic Liquids Containing Imidazolium Rings Interpreted Using Regular Solution Theory. *Ind. Eng. Chem. Res.* **2005**, *44*, 1928–1933.

(46) Camper, D.; Becker, C.; Koval, C.; Nobel, R. Diffusion and Solubility Measurements in Room Temperature Ionic Liquids. *Ind. Eng. Chem. Res.* **2006**, *45*, 445–450.

(47) Letcher, T. M.; Marciniak, A.; Marciniak, M.; Domanska, U. Activity Coefficients at Infinite Dilution Measurements for Organic Solutes in the Ionic Liquid 1-Hexyl-3-methylimidazolium Bis(trifluoromethylsulfonyl)imide Using g.l.c. at $T = (298.15, 313.15, \text{and } 333.15)$ K. *J. Chem. Thermodyn.* **2005**, *37*, 1327–1331.

(48) Kumelan, J.; Perez-Salado Kamps, A.; Tuma, D.; Maurer, G. Solubility of CO_2 in the Ionic Liquid [hmim][Tf_2N]. *J. Chem. Thermodyn.* **2006**, *51*, 1364–1367.

(49) Shiflett, M. B.; Yokozeki, A. Solubility and Diffusivity of Hydrofluorocarbons in Room-Temperature Ionic Liquids. *AIChE J.* **2006**, *52*, 1205–1219.

(50) Heintz, A.; Casas, L. M.; Nesterov, I. A.; Emel'yanenko, V. N.; Verevkin, S. P. Thermodynamic Properties of Mixtures Containing Ionic Liquids. 5. Activity Coefficients at Infinite Dilution of Hydrocarbons, Alcohols, Esters, and Aldehydes in 1-Methyl-3-butylimidazolium Bis(trifluoromethylsulfonyl)imide Using Gas-Liquid Chromatography. *J. Chem. Eng. Data* **2005**, *50*, 1510–1514.

(51) Lee, B.-C.; Outcalt, S. L. Solubilities of Gases in the Ionic Liquid 1-N-Butyl-3-methylimidazolium Bis(trifluoromethylsulfonyl)imide. *J. Chem. Eng. Data* **2006**, *51*, 892–897.

(52) Heintz, A.; Verevkin, S. P. Thermodynamic Properties of Mixtures Containing Ionic Liquids. 6. Activity Coefficients at Infinite Dilution of Hydrocarbons, Alcohols, Esters, and Aldehydes in 1-Methyl-3-octylimidazolium Tetrafluoroborate Using Gas-Liquid Chromatography. *J. Chem. Eng. Data* **2005**, *50*, 1515–1519.

(53) ChemDraw, v. 8.0; CambridgeSoft, 2003.

(54) Hyperchem, v. 7.01; Hypercube Inc.: Gainesville, FL, 2002.

(55) Codessa Pro, v. 1.0; University of Florida: Gainesville, FL, 2002.

(56) Katritzky, A. R.; Mu, L.; Lobanov, V. S.; Karelson, M. Correlation of Boiling Points with Molecular Structure. A Training Set of 298 Diverse Organics and a Test Set of 9 Simple Inorganics. *J. Phys. Chem.* **1996**, *100*, 10400–10407.

Received for review October 18, 2007. Accepted February 20, 2008.

JE700607B